# Investigation of Spaceflight Associated Neuro-Ocular Syndrome Asymmetry through Asymmetric Cranial Venous Modeling

Michael Van Akin[1]
*University of Colorado Boulder, Boulder, Colorado, 80309, USA*

Jay Buckey[2]
*Dartmouth College, Lebanon, NH, 03755, USA*

Danielle Carroll[3]
*University of Colorado Boulder, Boulder, Colorado, 80309, USA*

*and*

Allison Anderson[4]
*University of Colorado Boulder, Boulder, Colorado, 80309, USA*

**The Spaceflight Associated Neuro-ocular Syndrome (SANS) often presents with asymmetrical ocular structural changes, including asymmetric optic disc edema. The pathophysiology of these asymmetric SANS findings is unknown. Asymmetric pressure changes within the perioptic subarachnoid space are theorized to cause these findings. Asymmetric venous sinuses near the orbits could potentially result in asymmetric pressure changes within the perioptic subarachnoid space. MRI studies of normal subjects show a dominance of venous flow through the right transverse sinus in 59% of cases and hypoplasia of the left sinus in 39% of cases, suggesting that the right transverse sinus is dominant in approximately 60% of the population. In this paper, we present research intended to increase the fidelity of a computational craniovascular model, to investigate the role of cranial venous pathway asymmetry in SANS findings more effectively. The computational craniovascular lumped-parameter model was previously developed by Creare, LLC in collaboration with the Geisel School of Medicine at Dartmouth College. The model predicts changes to the structure and function of the cranial venous system in response to hydrostatic gradients, fluid shifts, and tissue weight changes. The model includes a circulatory sub-model, a cerebrospinal fluid sub-model, and an aqueous humor sub-model, but only includes a single venous drainage pathway. This limits its usefulness for studying asymmetric venous pathways and their effects on SANS. The model was modified to increase the number of lumped-parameter compartments in the cranial venous pathways and to model cranial venous pathways bilaterally instead of with a single pathway. Asymmetries will be introduced into the geometry of the modeled, bilateral venous sinuses to investigate their role in the development of asymmetrical ocular findings in microgravity.**

[1] PhD Student, Ann and H.J. Smead Department of Aerospace Engineering Sciences, 3775 Discovery Drive, Suite 224, 429 UCB – Aerospace, Boulder, CO 80303
[2] Professor of Medicine, Geisel School of Medicine at Dartmouth, One Medical Center Drive, Lebanon, NH 03756
[3] Physician, Department of Surgery, University of California San Francisco, 513 Parnassus Ave, S-321, San Francisco, CA 94143.
Graduate Student, Ann and H.J. Smead Department of Aerospace Engineering Sciences, 3775 Discovery Drive, 429 UCB – Aerospace, Boulder, CO 80303.
[4] Assistant Professor, Ann and H.J. Smead Department of Aerospace Engineering Sciences, 3775 Discovery Drive, AERO N303, 429 UCB – Aerospace, Boulder, CO 80303.

## Nomenclature

| | | |
|---|---|---|
| C | = | capacitance |
| $D$ | = | vessel diameter, subscript R for right, subscript L for left |
| $f$ | = | Darcy friction factor, subscript R for right, subscript L for left |
| $L$ | = | vessel length, subscript R for right, subscript L for left |
| $K$ | = | square root of the ratio of vessel resistances |
| $g$ | = | gravitational acceleration |
| $P$ | = | static or stagnation pressure, subscript D for downstream, subscript g for gravity induced, subscript U for upstream, |
| $R$ | = | fluid flow resistance, subscript R for right, subscript L for left, subscript v for total cranial venous |
| $r_{fv}$ | = | empirical constant for cranial venous compliance estimation |
| $Q$ | = | volumetric flow rate, subscript R for right, subscript L for left |
| $V$ | = | fluid velocity |
| $\alpha_{fv}$ | = | empirical constant for cranial venous compliance estimation |
| $\theta$ | = | angle relative to gravity vector |
| $\rho$ | = | fluid density |

## I. Introduction

Between 38% and 51% of astronauts on long-duration missions develop a collection of visual signs and symptoms collectively known as the spaceflight associated neuro-ocular syndrome (SANS).[1] Clinically, SANS is defined by the presence of optic disc edema[2], but there are other associated ocular responses including globe flattening, choroidal and retinal folds, hyperopic refractive error shifts, and nerve fiber layer infarcts[3]. These vision problems, if they are not correctable or progress, may jeopardize deep space mission objectives and crew safety.[1] The pathophysiology of SANS is currently unknown[3], but seems to be a unique effect of long-duration microgravity exposure.[3]

Asymmetric optic disc edema may be a characteristic of SANS based on astronaut ocular findings[1,2]. Unilateral ocular changes, including one-sided optic disc edema, have been observed in astronauts participating in long duration spaceflight.[2] Asymmetric pressure changes within the perioptic subarachnoid space are theorized to cause these unilateral SANS findings[2]. An asymmetry of venous drainage through the sinuses near the orbits could result in asymmetric pressure changes within the perioptic subarachnoid space[3]. Previous MRI studies of normal subjects have shown a dominance of venous flow through the right transverse sinus in 59% of subjects and hypoplasia of the left sinus in 39% of subjects[4,5], suggesting right transverse sinus dominance in approximately 60% of the population[3]. As a result, the asymmetry in transverse sinuses has been hypothesized to result in asymmetric optic disc edema during spaceflight.[2,3]

To investigate the role of asymmetry in the cranial venous pathways, we augmented a lumped-parameter craniovascular model developed by Creare, LLC and Dartmouth College. Prior to this work, only a single cranial venous pathway between the cranial capillaries and the jugular veins or vertebral plexus was implemented. Through the addition of a higher fidelity, bilateral breakdown of sinuses within the cranial venous pathways, we can isolate the potential acute ocular changes resulting from asymmetries in anatomical geometry.

## II. Fundamental Fluid Mechanics Applied to the Cranial Venous System

Current hypotheses suggest that pressure asymmetries in the perioptic subarachnoid space result in asymmetrical SANS findings.[2,3] Perioptic subarachnoid asymmetries are expected to occur from pressure asymmetries in the cerebral veins.[2,3] To understand the pressure effects of anatomical asymmetry in the cranial venous system, we document the predicted effects from a fundamental fluid dynamics perspective. In the cranial venous system, blood flows through the superior sagittal sinus and then through two parallel sets of cranial venous pathways. A current hypothesis in the SANS community is that a larger transverse sinus may cause cranial venous pooling, resulting in a higher-pressure environment in the right venous system as compared to the left venous system.[2,3] To investigate this hypothesis conceptually, we first simplify the venous system into the parallel pipes shown in Figure 1a, where the inflow represents the superior sagittal sinus, the parallel paths represent the cranial venous system, and the outflow represents the drainage of the jugular veins into the superior vena cava. The variable P represents the pressure head upstream ($P_U$) and downstream ($P_D$) of the cranial venous system. The variable R represents the resistance of each parallel path, Q represents the volumetric flow rate through each pathway, and D represents the diameter of each path, assuming each has a circular cross-sectional area.

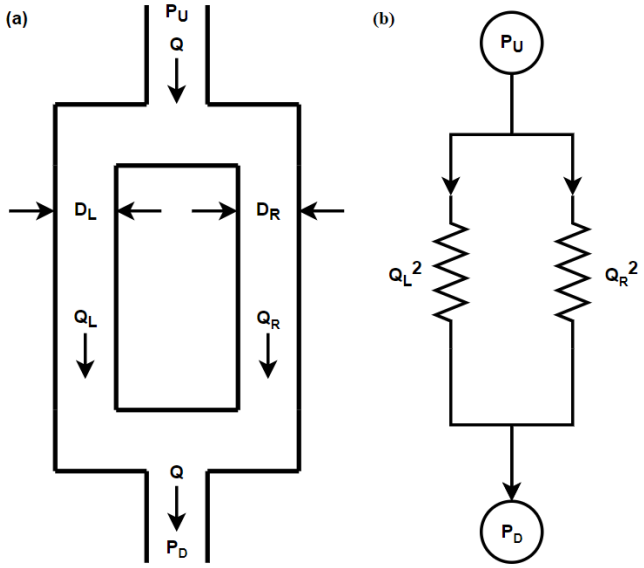


Figure 1. (a) Fluid flow diagram for flow through parallel pipes as an analogy for bilateral cranial venous pathways. (b) Equivalent electric network system for fluid flow through parallel pipes

Figure 1b shows an equivalent electric network system for fluid flow through parallel pipes. The resistance of a pipe in a fluid flow system is calculated using Equation 1[6] for laminar, inviscid flow, where L is the length, D is the diameter, g is the gravitational acceleration and f is the Darcy friction coefficient.

$$R = \frac{8L}{\pi^2 D^5 g} f \tag{1}$$

To equate a fluid flow system and electric system, the volume flow rate is squared in order to be proportional to an analogous current. The volume flow rate and pressure head difference are calculated using Equations 3 through 5, where Q represents the volume flow rate through each parallel pipe, K is the square root of the ratio of resistance of the parallel pipes calculated in Equation 2, and V is the fluid velocity. Subscripts L and R are used to distinguish fluid flow parameters of the left- and right-sided fluid pathways, respectively.

$$K = \sqrt{\frac{R_R}{R_L}} \tag{2}$$

$$Q_L = \frac{K}{1+K} Q, \;\; Q_R = \frac{1}{1+K} Q, \;\; Q = Q_R + Q_L \tag{3}$$

$$P_U - P_D = \frac{f_L L_L V_L^2}{2 D_L g} = \frac{f_R L_R V_R^2}{2 D_R g} \tag{4}$$

Equation 5 is derived from Equation 4, substituting fluid velocity and cross-sectional area for the volumetric flow rate. These equations again assume a circular cross-sectional area.

$$P_U - P_D = \frac{8 L_L}{\pi^2 D_L^5 g} f_L Q_L^2 = \frac{8 L_R}{\pi^2 D_R^5 g} f_R Q_R^2 \tag{5}$$

The kinetic energy traveling through each parallel pipe will be split between organized and random motion. This can be represented with dynamic and static pressure; both of these contribute to the increased stagnation pressure, which is conserved for incompressible flow. The stagnation pressure calculation, assuming no height changes, is shown in Equation 6, using the static pressures calculated in Equation 5.

$$P_{stagnation} = P_{static} + \frac{1}{2} \rho V^2 \tag{6}$$

If a larger right transverse sinus caused an increase in perioptic subarachnoid pressure because of fundamental fluid dynamics, we would expect to see elevated venous pressure through the right transverse sinus. MATLAB was used to calculate the effects of varying the ratio of diameters on the static pressure in each parallel pipe. The lengths and friction coefficients of the pipes were set to be identical to represent cranial veins whose only difference is the cross-sectional area (i.e., an asymmetric anatomy), although different Reynold's numbers in the parallel pipes would affect the friction coefficients. We set the upstream gauge pressure to 106.4 Pa and the atmospheric pressure to 101,325 Pa as was implemented in the Creare craniovascular model. We also set the fluid density to 1,000 kg/m$^3$ as the density of blood is assumed to be close to that of water[7], the upstream diameter to 0.01 m based on experimental MRI data collected by this research team, as described in Section III, and the upstream flow rate to 14 mL/s, as was implemented in the Creare craniovascular model. These assumptions allow the ratio of volume flow rates and the ratio of fluid velocities to be calculated using only one input, a diameter ratio. All ratios represent the ratio of the fluid parameter in the larger-diameter side (right) divided by the fluid parameter in the smaller-diameter side (left). Note that this notation was chosen because dominance of the right transverse sinus over the left is more commonly found in the general population and this allows for diameter ratios greater than or equal to one, but there is no mathematical significance of assigning the left or right sided dominance. This diameter ratio represents varying degrees of anatomical asymmetry in cross-sectional area. Static pressure cannot be calculated with only a diameter ratio, however. To calculate a ratio of static pressures, the assumptions listed above for the upstream pressure, atmospheric pressure, fluid density, upstream diameter, and upstream flowrate are needed. The effects of diameter ratio on pressure ratio, volume flow rate ratio, and fluid velocity ratio are shown in Figures 2a, 2b, and 2c respectively. We input diameter ratios up to four (i.e., the diameter of the right side was four times as large as the left side).

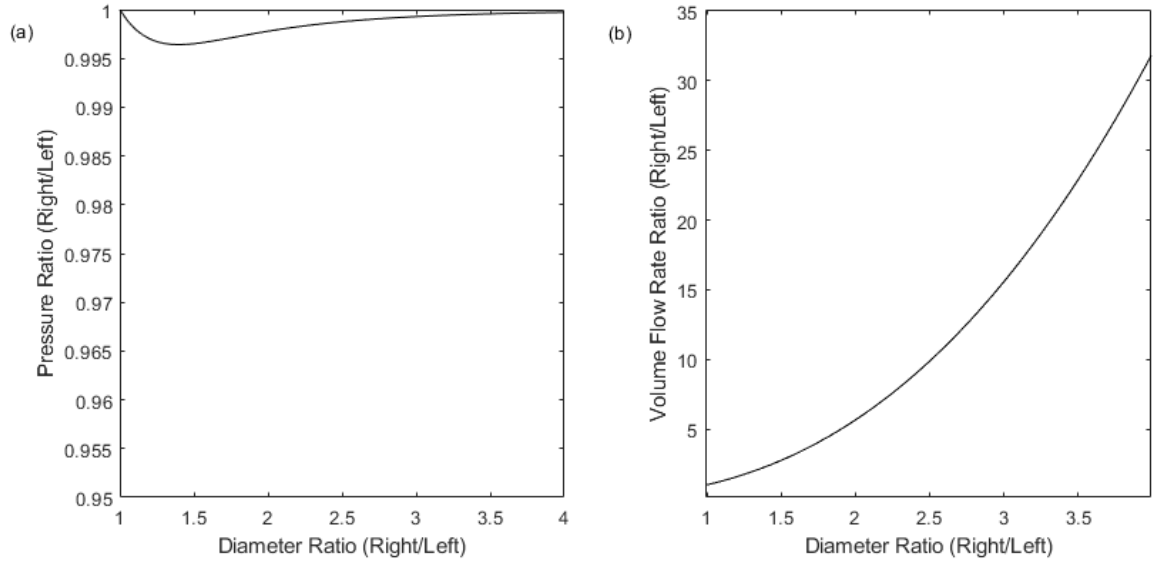


Figure 2. Ratio of fluid parameter ratios (right/left) vs diameter ratio (right/left) (a) Pressure ratio vs diameter ratio (b) Volume flow rate ratio vs diameter ratio (c) Velocity ratio vs diameter ratio (on next page)

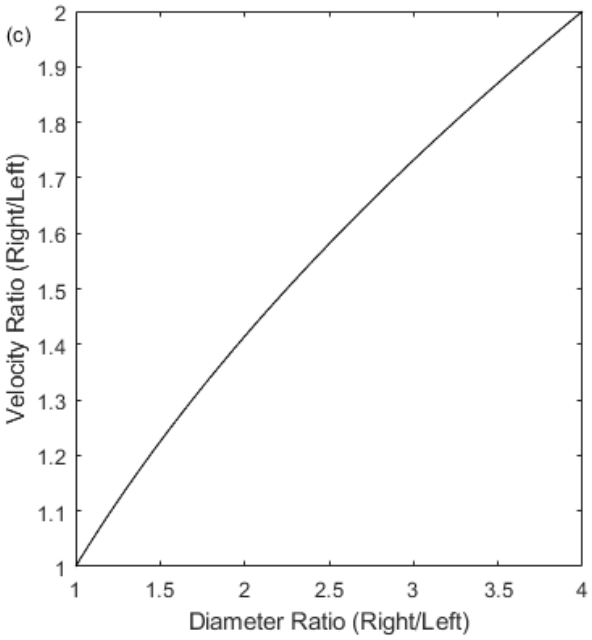


Figure 2. Ratio of fluid parameter ratios (right/left) vs diameter ratio (right/left) (a) Pressure ratio vs diameter ratio (on previous page) (b) Volume flow rate ratio vs diameter ratio (on previous page) (c) Velocity ratio vs diameter ratio

The outputs of this simplified model demonstrate that volume flow rate increases in the larger vessel as the diameter is increased, as shown in Figure 2b. This is expected, as in an equivalent electric system, the current increases through the parallel branch with a lower resistance. The larger diameter decreases the fluid flow resistance through the larger side. The fluid velocity also increases through the larger side because of the volume flow rate increasing faster than the cross-sectional area of the larger side, as shown in Figure 2C. Figure 2A shows that the static pressure in the larger side decreases compared to the smaller side, although this difference is less than 0.5%. In fact, to identify the change, the y-axis range is scaled to represent a 5% change and fluctuation is only minimally visible. This decrease converges back to unity as the diameter ratio increases. These results have a bearing on the current hypothesis suggesting that a dominant right transverse sinus leads to the observed right sided dominance of asymmetrical SANS findings.[2,3] The larger right side diameter does not yield a right side pressure increase using fundamental fluid dynamics. However, given the significant limitations of this simplified model, a higher fidelity model is needed to understand if there is a causal link between right sided venous drainage dominance and predominance of SANS findings in the right eye. This may elucidate whether effects beyond fundamental fluid dynamics, including venous pooling, can be captured with a higher fidelity representation of craniovascular anatomy.

## III. Higher Fidelity Craniovascular Model

### A. Model Description

A computational craniovascular lumped-parameter model was previously developed by Creare, LLC in conjunction with the Geisel School of Medicine at Dartmouth College (http://weightless.dartmouth.edu/). This Simulink/MATLAB model predicts changes to the structure and function of the cranial venous system in response to hydrostatic gradients, fluid shifts, and changing tissue properties. The model, includes a circulatory sub-model, a cerebrospinal fluid (CSF) sub-model, and an aqueous humor sub-model[8]. The sub-models interact through pressure boundaries and indirect fluid transfer mechanisms of a single "working fluid"[8].

This research builds from this model to provide additional fidelity to the cranial venous component of the model. The inputs to the model include posture as a function of simulation time, lower body pressure as a function of simulation time, and gravity level as a function of time. The head veins section of the circulatory sub-model is the portion of the model augmented in this research. Flow from the head capillaries and eye sections of the model serve

as inputs to the head veins, following the anatomical flow. Flow exits the head veins blocks as inputs to the jugular vein and vertebral plexus blocks.

Cranial venous fluid flow is modeled as shown in the equivalent electrical diagram in Figure 3. This figure represents the components needed to model the behavior of each vessel in response to pressure, volume, and flow rate changes. Each equivalent electrical component is defined using vessel geometries and vessel wall properties. Starting with the flow source in Figure 3, the fluid entering a vessel encounters a resistance to flow, and then a pressure increase due to gravitationally induced hydrostatic gradients. The vessel volume then responds to the fluid inflow pressure, modeled as the compliance of the vessel. The compliance changes the vessel volume according to the difference in vessel pressure and external pressure.

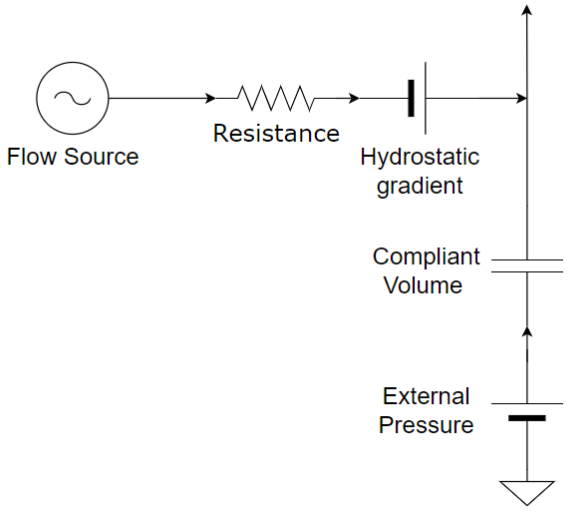


Figure 3. Equivalent electrical diagram for single cranial vein lumped parameter fluid compartment (flow source, flow resistance, hydrostatic gradient pressure addition, compliant volume, and external pressure modeled)

The original cranial veins electrical equivalent diagram is shown in Figure 4. Flow enters the head veins block from the capillaries, shown at the left of Figure 4. This upstream flow source encounters a resistance to flow due to the cross-sectional area and length of the head veins. This results in a pressure drop as the flow passes through veins. Total venous flow is modeled with resistances at the venules, small head veins, and the large head veins. As such, no specific vessels are modeled. The compliance component changes the volume of the veins according to pressure environment from the capillaries, cerebrospinal fluid (CSF) which causes the external pressure, and aqueous humor (AH) fluid flow from the eyes. The head vein volume responds to changes in fluid pressure depending on the vein's compliance. Finally, a gravitationally induced hydrostatic gradient changes the pressure of the fluid, increasing in the direction of the gravity vector. In this model, the gravitationally induced hydrostatic pressure increase is modeled after all resistance blocks and is dependent on the gravitational acceleration and posture of the person. Flow is then directed either to a single jugular vein or to the vertebral plexus through a Simulink data structure that stores several fluid properties, including pressure and flow rate. The craniovascular model currently accommodates supine and prone postures, as the tissue weights and hydrostatic gradients for these postures are included in the model.

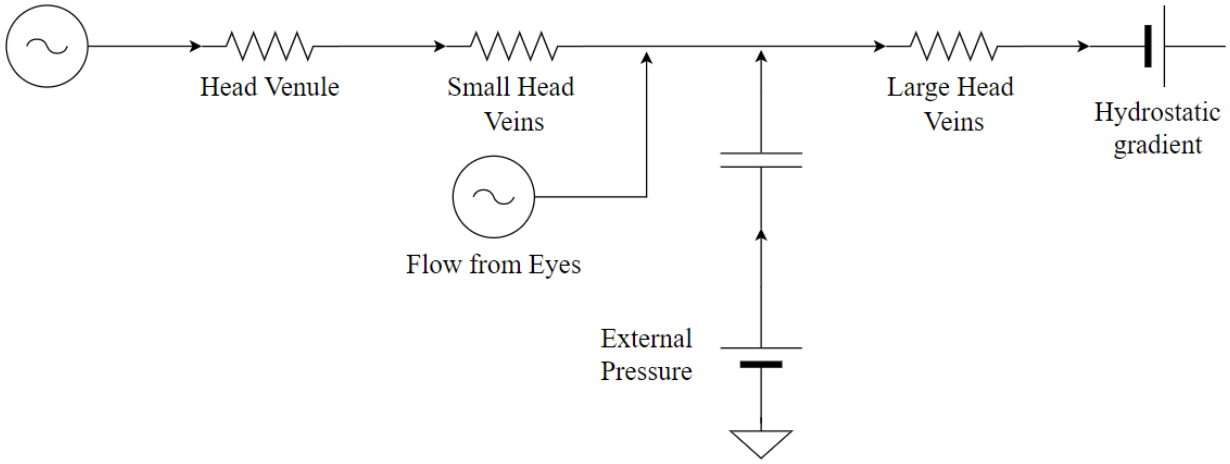


Figure 4. Original cranial veins equivalent electrical diagram (flow sources, flow resistances, hydrostatic gradient pressure addition, compliant volume, and external pressure modeled)

Figure 4 shows the limitations of the current Creare craniovascular model in investigating anatomical asymmetry effects on ocular findings. There is only a single pathway of blood flow through the cranial venous system, and the breakdown of resistances is not sufficient to model individual vessel asymmetry, in particular, transverse sinus asymmetry. In this research, we present augmentations to include bilateral pathways and a partitioning of resistances based on individual cranial venous sinus anatomy.

**B. Vessel Selection**

Modifications were made to the model to increase the number of lumped-parameter compartments in the head veins and to model cranial venous pathways bilaterally, instead of with a single pathway, as was used previously. Asymmetries can be introduced into the geometry of the bilateral venous sinuses to investigate their role in the development of asymmetrical ocular findings in microgravity. An equivalent electrical diagram for these bilateral pathways is shown in Figure 5 and includes the superior sagittal sinus, the transverse sinuses, the cavernous sinuses, and sigmoid sinuses. These vessels were selected for incorporation as pathways that may have a substantial effect on venous flow.[3,9] In the future, we plan to include ancillary resistances along these pathways to further improve fidelity, including the superior and inferioranastomotic veins, the superior and inferior petrosal sinuses, and the occipital sinus. A critical addition of improvement included in this model is the addition of bilateral pathways, as this is a core aspect of understanding bilateral changes. Figure 5 shows only one side of the bilateral model, excluding that the superior sagittal sinus, which is the only vessel added to the model that is unilateral, since it is a single fluid pathway.

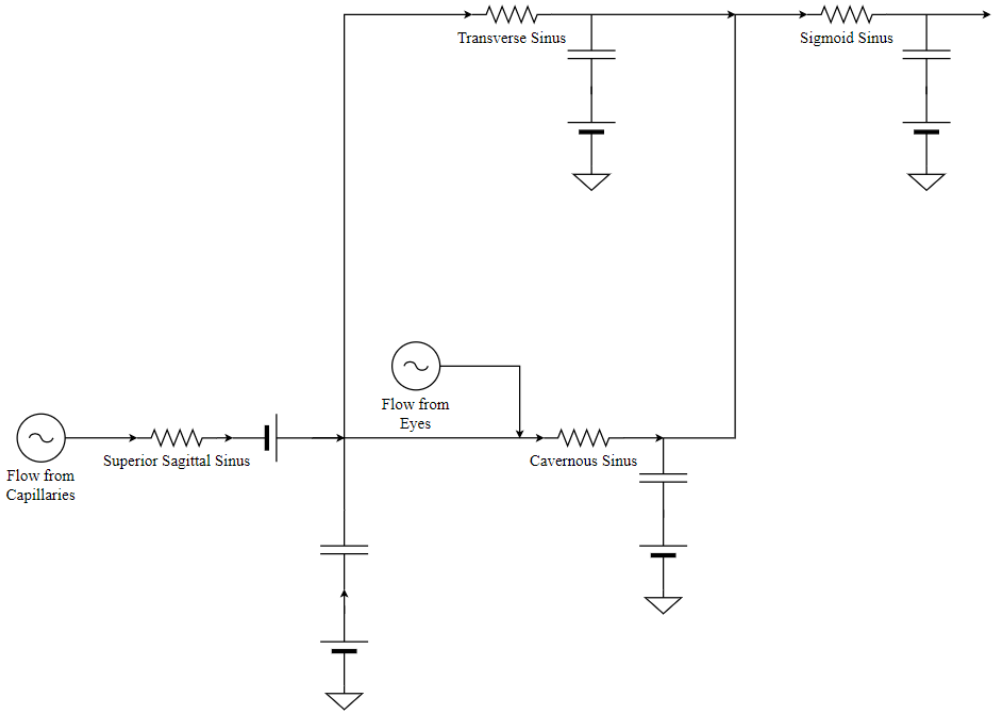


Figure 5. Equivalent electrical diagram for single side of augmented model

### C. Parameters

To understand the effects of anatomical variants and asymmetry on SANS findings, the aforementioned, higher fidelity and bilateral vessel model will be modified to incorporate parameters representing asymmetric geometry. To define the resistances, hydrostatic gradients and capacitance of each vessel shown in Figure 5, several anatomic geometries of these vessels are needed. This resistance for each vessel can be determined from the length and diameter using Equation 1, where *f*, the Darcy Friction factor, can be determined from the flow's Reynolds number. The hydrostatic pressure added after each resistance is calculated using Equation 7 and requires the vessel length and angle relative to the gravitational vector. With the posture input from the model, this angle can be found knowing the angle of the vessel relative to an axis of the body.

$$P_g = \rho g L cos\theta \tag{7}$$

Specific vessel capacitances were not identified in the literature. Rather, total capacitance has been experimentally calculated[10]. To derive a vessel-specific capacitance, we follow a method derived from Lakin et al. The authors detail a process for determining the capacitance of individual veins and sinuses for lumped parameter models, requiring a breakdown of volume by vessel. First, an overall capacitance, $C_{fv}^4$ is calculated for the CSF/cranial venous boundary using Equation 8, where $C_{fv}^O$, r and α are empirical constants calculated by Lakin et. al. The overall capacitance responds to the pressure across the vessel volume, $P_{fv}$ and plateaus according to rigid volume boundaries. This capacitance can be divided further into more specific lumped parameters using ratio of volumes. Each vein/sinus is assigned a percentage of the overall capacitance based on the percentage of the entire volume that each vein/sinus occupies.[10]

$$C_{fv}^4(P_{fv}) = C_{fv}^O e^{-r_{fv}|P_{fv}|^{\alpha_{fv}}} \tag{8}$$

There is little information in the literature regarding individual cranial venous vessel geometries as is required for the lumped-parameter model. Therefore, to define vessel resistances (which depend on vessel lengths and diameters), hydrostatic gradients (which depend on vessel lengths and angle to the body reference frames), and capacitances, experimental data are needed.

### D. Experimental Data Incorporation

To derive anatomical values for cranial veins and sinuses, experimental MRI data will be segmented. An experiment was conducted in the Space Medicine Innovations Lab at the Giesel School of Medicine at Dartmouth College to study the acute effects of lower body negative and positive pressure (LBNP/LBPP) and posture on the eye. Subjects' seated baseline ocular and MRI data were collected upon entering the laboratory. All subsequent experimental conditions (supine atmospheric, supine LBPP, supine LBNP, prone atmospheric, prone LBPP, prone LBNP) were ordered randomly for each subject. Upon entering each condition, a 15-minute rest interval prior to data collection was used to achieve approximate homeostasis. LBNP/LBPP was administered using a custom-built MRI-compatible chamber. The data collected in this study were originally used to tune and validate the original craniovascular model built by Creare and Dartmouth, but specific venous anatomies were not calculated nor incorporated in the model. As such, this same data set will be used to define geometries of the vessels in order to determine the resistance, which can then be used to tune and validate our bilateral model to match experimentally derived outputs.

Baseline supine values for the length, cross-sectional area, and volume of the superior sagittal sinus, transverse sinus, and sigmoid sinus were determined through segmentation of magnetic resonance venography (MRV) data collected in the study previously described. The free software-tool, ITK-SNAP (University of North Carolina at Chapel Hill) was used to perform this segmentation on the previously described MRI data. The snake automatic segmentation tool was used to find the volume, cross-sectional area, and length of cranial venous pathways. These pathways were split into individual vessels, the superior sagittal sinus, the transverse sinuses, and the sigmoid sinuses, using the 3D scalpel tool. This process is modeled from a previous study with sinus segmentation[11]. An example of the resulting segmentation is shown in Figure 1b of Rohr et al.[11]

### E. Model Tuning and Validation

The original Creare craniovascular model was tuned and validated with MRI data from studies conducted at the Geisel School of Medicine. Supine MRI and MRV velocimetry data from 12 test subjects including anatomical geometries and observed vessel flow rates were used to tune the model to output results similar to those seen in the experimental supine posture. There are few literature values for vessel resistances and compliances, thus these were initially used as tuning parameters to achieve flow rates and other observable metrics found in laboratory studies. The model was then validated in the other experimental conditions that included the prone posture and LBNP and LBPP in both the supine and prone postures. Intraocular pressure, carotid and jugular flow rates, and diastolic pressure were used to compare experimental and validated model outputs. Jugular flow rates are shown in Figure 6 as an example of this validation.[12]

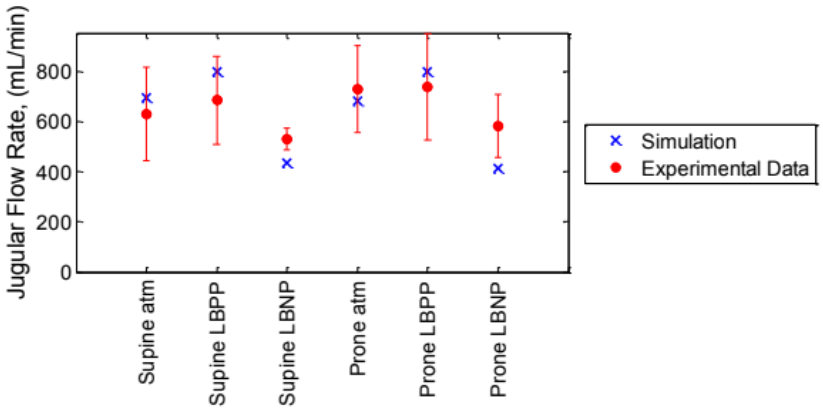


Figure 6. Jugular Flow Rate Model Validation in Experimental Conditions[12]

In this research effort, we will pursue a similar validation methodology. The updated, bilateral cranial venous model will be tuned to output flow rates and pressures in the jugular vein close to those values in the original model. We have yet to develop a process for finding anatomical geometries of the cavernous sinuses, so the resistance, hydrostatic gradients, and compliance for these vessels will be tuned through an iteration of reasonable vessel lengths and volumes.

Cranial venous resistances derived from MRV geometric measurements of sinuses can be compared to the overall cranial venous resistance calculated by Schulman et al. using Equation 9.[6] With the fundamental equivalent electrical resistance shown in Equation 10 and the calculated sinus resistances in Equation 1, we can compare overall cranial

venous resistances. The difference in these calculations may lead to discrepancies. Additionally, differences in overall resistance calculations may result from our exclusion of ancillary vessels. These smaller, ancillary vessels provide a high resistance, and as a result, the flow rate through them is substantially less than larger vessels. Therefore, the inclusion of these vessels is not a priority for the first iteration of a bilateral cranial venous model, despite potential discrepancies in overall resistance.

$$R_v = \frac{subarachnoid\ venous\ pressure - \ venous\ outflow\ pressure}{venous\ flow\ rate} \tag{9}$$

$$R_{parallel} = \frac{R_1 R_2}{R_1 + R_2}, R_{series} = R_1 + R_2 \tag{10}$$

## IV. Conclusion

We have developed a computational method of evaluating the effect of anatomical asymmetries in the cranial venous pathways on SANS findings. We first clarify how anatomical asymmetry does not yield asymmetric pressures from a simple, first principles fluid flow model. We then outline the method by which a higher fidelity model will be used to investigate these hypotheses in an anatomically relevant manner. Cranial venous model fidelity will be improved with the inclusion of bilateral pathways with an increased number of lumped parameters that are defined with experimentally derived anatomical and fluid flow data. Modeled acute changes can be used to inform potential long-term mechanisms that cause asymmetry in SANS findings. Our research using fundamental fluid dynamics principles suggests that a dominant right transverse sinus would not result in the increase in right perioptic subarachnoid space pressure expected to cause SANS asymmetries. Future research will need to address why right dominance in the transverse sinus may be associated with more SANS findings in the right side.

## Acknowledgments

The authors would like to thank their research participants for engaging in the study. This work was supported by grant CA03401 and PF04103 from the National Space Biomedical Research Institute through NCC 9–58, by NASA EPSCoR Cooperative Agreement NNX13AD35A, and by a National Science Foundation Graduate Research Fellowship. The authors would also like to acknowledge Creare, LLC. for the development of the original model from which this research is based, specifically Scott Phillips, Darin Knaus, Veronique Archambault-Leger, and Ariane Chepko. We thank Abigail Fellows and Kseniya Masterova for their help in collecting the baseline data used to build the model.

## References

*Reports, Theses, and Individual Papers*

[1]Mader TH, Gibson CR, Pass AF, et al. Optic Disc Edema, Globe Flattening, Choroidal Folds, and Hyperopic Shifts Observed in Astronauts after Long-duration Space Flight. *Ophthalmology*. 2011;118(10):2058-2069. doi:10.1016/j.ophtha.2011.06.021

[2]Mader TH, Gibson CR, Otto CA, et al. Persistent Asymmetric Optic Disc Swelling After Long-Duration Space Flight: Implications for Pathogenesis. *Journal of Neuro-Ophthalmology*. 2017;37(2):133-139. doi:10.1097/WNO.0000000000000467

[3]Aintablian H, Fleischer J, Brunstetter T, Tarver WJ. Spaceflight Associated Neuro-Ocular Syndrome: A Mechanism for the Unilateral Tendencies. *89th Annual ASMA Scientific Meeting*.

[4]Ayanzen RH, Bird CR, Keller PJ, McCully FJ, Theobald MR, Heiserman JE. Cerebral MR Venography: Normal Anatomy and Potential Diagnostic Pitfalls. *Am J Neuroradiol*. 2000;21(1):74.

[5]Scotti G, Yu C, Dillon W, et al. MR imaging of cavernous sinus involvement by pituitary adenomas. *American Journal of Roentgenology*. 1988;151(4):799-806. doi:10.2214/ajr.151.4.799

[6]Shulman K, Verdier G. Cerebral vascular resistance changes in response to cerebrospinal fluid pressure. *American Journal of Physiology-Legacy Content*. 1967;213(5):1084-1088. doi:10.1152/ajplegacy.1967.213.5.1084

[7]Kenner T. The measurement of blood density and its meaning. *Basic Res Cardiol*. 1989;84(2):111-124. doi:10.1007/BF01907921

[8]Buckey JC, Phillips SD, Anderson AP, Cowan DR. The Importance of Tissue Weight and Tissue Compressive Forces in Human Spaceflight. *68th International Astronautical Congress (IAC)*.

[9]Byrne JV. Cranial Venous Anatomy. In: *Tutorials in Endovascular Neurosurgery and Interventional Neuroradiology*. Springer Berlin Heidelberg; 2012:53-69. doi:10.1007/978-3-642-19154-1_3

[10]Lakin WD, Stevens SA, Tranmer BI, Penar PL. A whole-body mathematical model for intracranial pressure dynamics. *Journal of Mathematical Biology*. 2003;46(4):347-383. doi:10.1007/s00285-002-0177-3

[11]Rohr A, Bindeballe J, Riedel C, et al. The entire dural sinus tree is compressed in patients with idiopathic intracranial hypertension: a longitudinal, volumetric magnetic resonance imaging study. *Neuroradiology*. 2012;54(1):25-33. doi:10.1007/s00234-011-0850-6

[12]Lu R. Essential Parameters for Modeling Space-Induced Visual Changes. https://weightless.dartmouth.edu/publications/